Transcriptional analysis of nasal polyps fibroblasts reveals a new source of pro-inflammatory signaling in CRSwNP*

C. Porras-González[1,2,§,†], J.M. Palacios-García[1,§], S. Sánchez-Gómez[1,2], J.M. Maza-Solano[1,2], G. Alba[3], V. Sánchez-Margalet[3], O. Palomares[4], A. Del Cuvillo[5], J.A. Cordero-Varela[6], R. Moreno-Luna[1,2,†], J.L. Muñoz-Bravo[7]

[1] Rhinology Unit, Department of Otolaryngology, Head and Neck Surgery, Virgen Macarena University Hospital/FISEVI, Seville, Spain

[2] Institute of Biomedicine of Seville (IBiS), Virgen del Rocío University Hospital, University of Seville, CSIC, Seville, Spain

[3] Department of Medical Biochemistry, Molecular Biology and Immunology, School of Medicine, Virgen Macarena University Hospital, University of Seville, Seville, Spain

[4] Department of Biochemistry and Molecular Biology, School of Chemistry, Complutense University of Madrid, Madrid, Spain

[5] Rhinology and Asthma Unit, ENT Department, University Hospital of Jerez, Jerez de la Frontera, Cadiz, Spain

[6] Bioinformatics and Computational Biology Facility, Institute of Biomedicine of Seville (IBiS), Virgen del Rocío University Hospital, University of Seville, CSIC, Seville, Spain

[7] Clinical Analysis Service, General University Hospital of Elche, Alicante. Foundation for the Promotion of Health and Biomedical Research in the Valencia Region (FISABIO), Valencia, Spain

[§] Both authors contributed equally

[†] Both authors are corresponding authors

Rhinology 61: 2, 180 - 189, 2023

https://doi.org/10.4193/Rhin22.309

***Received for publication:** August 18, 2022

Accepted: January 16, 2023

Abstract

Background: Fibroblasts and others mesenchymal cells have recently been identified as critical cells triggering tissue-specific inflammatory responses. Persistent activation of fibroblasts inflammatory program has been suggested as an underlying cause of chronic inflammation in a wide range of tissues and pathologies. Nevertheless, the role of fibroblasts in the emergence of chronic inflammation in the upper airway has not been previously addressed. We aimed to elucidate whether fibroblasts could have a role in the inflammatory response in chronic rhinosinusitis with nasal polyps (CRSwNP).

Methodology: We performed whole-transcriptome microarray in fibroblast cultured from CRSwNP samples and confirmed our results by qRT-PCR. We selected patients without other associated diseases in upper airway. To investigate shifts in transcriptional profile we used fibroblasts from nasal polyps and uncinate mucosae from patient with CRSwNP, and fibroblasts from uncinate mucosae from healthy subjects as controls.

Results: This study exposes activation of a pro-inflammatory and pro-fibrotic transcriptional program in nasal polyps and CRSwNP fibroblasts when compared to controls. Our Gene-set Enrichment Analysis (GSEA) pointed to common up-regulation of several pro-inflammatory pathways in patients-derived fibroblasts, along with higher mRNA expression levels of cytokines, growth factors and extracellular matrix components.

Conclusions: Our work reveals a potential new source of inflammatory signaling in CRSwNP. Furthermore, our results suggest that deregulated inflammatory signaling in tissue-resident fibroblasts could support a Type-2 inflammatory response. Further investigations will be necessary to demonstrate the functionality of these novel results.

Key words: gene expression, inflammation, NPDF, rhinosinusitis, Type-2 immune response

Introduction

Fibroblasts have emerged recently as sentinels of tissue homeostasis, integrating damage signals and immune responses (for a recent review see [(1)]). A growing body of evidence supports a major role for fibroblasts, and other innate immune cells, in the emergence of tissue-specific chronic inflammation [(2,3)]. Upon activation by stress signals tissue-resident fibroblasts alter their chromatin dynamics, transitioning to an active-state. These ac-

tive fibroblasts are reprogrammed to respond exaggeratedly to secondary immunological challenges or stress signals, thereby rendering the tissue prone to inflammation [4]. Deregulated activation of fibroblast by stress signals is a common step in inflammatory diseases from different tissues that leads to deterioration in the condition [5]. Interestingly, some shared features underpin active fibroblasts transcriptional program. Chiefly, inflammatory signaling in fibroblasts is utterly associated with production of extracellular matrix (ECM) components and metalloproteases, secretion of growth factors for tissue remodeling, and cytokines to modulate tissue-specific immune responses [1]. Moreover, recent data also points to increased metabolic activity, and a shift to normoxic glycolysis, as another sign of fibroblasts activation [2], essential to match their increased energy requirements. These stress-activated fibroblasts can preserve their transcriptional reprograming during generations both in vivo and in vitro, thus leading to sustained inflammation if not properly regulated. The precise mechanism is probably tissue-specific, although many authors have pointed to epigenetic modifications as drivers of this sustained inflammatory program [4,6,7].

Recent reports demonstrate that fibroblasts, and fibroblasts-like stromal cells are important mediators of type-2 immunity[8]. Lymphoid cells are usually found in close association with stromal cells, allowing them to engage in complex bi-directional communication, and to coordinate the immune response with signals from the surrounding tissue [9]. In fact, close association of fibroblasts with ILC2 and tissue-resident Th2 cells is evident in certain niches along the lower respiratory tract and many other tissues [3,10], suggesting a conserved mechanism of type-2 immune regulation. In these setting stress-activated fibroblasts are able to induce ILC2 and tissue-resident Th2 expansion and activation [8], and consequently support tissue-specific type-2 inflammatory immune responses when exposed to stress signals or immunological challenges. Indeed, fibroblasts have been implicated in inflammatory tissue priming in rheumatoid arthritis [2,3], a niche-specific regulatory mechanism with obvious implications in type-2 inflammatory diseases.

Chronic rhinosinusitis is a chronic inflammatory disease of the upper airway of unknown etiology, which vary in the severity of the presentation, and might give rise to nasal polyps (CRSwNP) [11]. CRSwNP exhibit an increasing type-2 inflammation-induced gene signature [12], which is thought to be a critical driver of the disease. Consequently, new biological treatments targeting type-2 cytokines ameliorate CRSwNP symptoms and reduce nasal polyps outgrow [13–15]. Upper airway is intrinsically exposed to repetitive immunological challenges, but the contribution of the fibroblasts to the deregulation of the type-2 inflammatory signaling in CRSwNP remains poorly understood. Genome-wide association studies (GWAS) have identified association of CRSwNP with several loci related to innate immune system, ECM and Th2 signalling [16,17]. CRSwNP is often associated to other respiratory pathologies, such as asthma, cystic fibrosis, aspirin intolerance, allergic processes and more. These associated diseases could indicate multiple etiologies of the CRSwNP and confounding additional mechanism triggering inflammation. Considering all these aspects, we hypothesized that stress-activated fibroblasts in CRSwNP could in part underlay the sustained type-2 inflammation reported in these patients. Therefore, we sought to elucidate their potential contribution to CRSwNP sustained inflammation by investigating transcriptional changes in fibroblasts from a selected subset of CRSwNP with unexplained underlying cause of dysfunction, and no history of any other respiratory disease. Herein, we uncover activation of a pro-inflammatory and pro-fibrotic transcriptional program in nasal polyps fibroblasts, thus pointing to CRSwNP fibroblast as possible contributors to sustained Type-2 inflammation in nasal polyps.

Materials and methods

Participant recruitment

Patients with CRSwNP diagnosed according to the EPOS 2020 international consensus criteria were included [18]. The radiological extension of the disease was evaluated by multislice computerized tomography using the Lund-MacKay Scored (LMS) [19]. Five patients candidates to endoscopic sinus surgery (ESS) and no previous history of asthma, allergic rhinitis, cystic fibrosis, chronic obstructive pulmonary disease (COPD) or aspirin-exacerbated respiratory disease (AERD), were selected. Three healthy subjects undergoing deviated septum surgery, with absence of sinusitis symptoms, endoscopic or radiological sinusitis findings were recruited as control group. Asthma, allergic rhinitis or AERD were diagnosed following Spanish Guide for the Management of Asthma GEMA [20] and Bousquet et al. criteria [21]. None of the patients was treated with monoclonal antibodies at least one year before surgery, nor with antihistamines, oral corticosteroids or antileukotrienes, at least three months before surgery.

The study was approved by the Research Ethics Committee of Hospitales Universitarios Virgen Macarena-Virgen del Rocio (projects PI-0212-2017 and PIGE-0367-2019). All participants included in this study signed an informed consent.

Isolation of samples and cell culture

Uncinate process mucosa (UM) was obtained from control subjects during septoplasty. UM and Nasal Polyps (NPs) tissue were collected from patients with CRSwNP through functional ESS. Fibroblasts were isolated as previously described [22]. Briefly, tissue was enzymatically disaggregated using collagenase (500 U/mL, Sigma), hyaluronidase (30 U/mL, Sigma) and DNase (10 U/mL, Sigma). The cell suspension was filtered at 70 µm, and erythrocytes were lysed with ACK buffer (GIBCO). For the experiment, cells were seeded at 10^4 cells/cm^2 in DMEN supplemented with 4% FBS, 1% P/S and 1% L-Glu. Cellular pellets were immediately

frozen in N_2 liquid and stored at -80ºC until RNA extraction.

RNA extraction

Total RNA extraction was carried out at the research support facility of the Institute of Biomedicine of Seville (IBiS) using the RNeasy Micro Kit 74004 (Qiagen), following the manufacturer's instructions. Determination of the RNA yield and purity was performed on a nanodrop 2000c spectrophotometer (Thermo Scientific).

Microarray

Microarray was performed at the Genomic facility of IBiS as reported previously [23]. Briefly, RNA quality was analysed using a 4200 Tapestation system (Agilent). Only samples with RNA integrity number (RIN) greater than 8 were used. 100ng of total RNA were amplified and labeled following manufacture instructions (GeneChip® WT PLUS Reagent Kit, Thermo Fisher Scientific, Inc). 5.5 µg of cDNA was used for hybridization to GeneChip Clariom S Human Array (Thermo Fisher Scientific, Inc.).

Data analysis

Transcriptome results were analysed in cooperation with the Bioinformatics and Computational Biology facility of IBiS. Affymetrix raw data was analysed using R statistical environment (RStudio, Inc.). Robust Multi-Array (RMA) method was used to perform data normalization. Analysis of differential gene-expression was performed with LIMMA/Bioconductor package and data quality was confirmed using Array Quality Metrics package. Only genes with a p-value of 0.05 and a fold change of ±1.5 were considered. Gene-set Enrichment Analysis (GSEA) software was used to identify underlying biological processes [24]. Only gene sets with an adjusted p-value (FDR) ≤ 0.05 and a normalized enrichment score (NES) of ≥ 1.40 or ≤ -1.40 were considered. Single-cell RNA sequencing data was obtained from Dahlgren et al. [8], and Boothby et al. [3] supplementary information.

Quantitative real time RT-PCR

ViiA 7 Real-Time PCR System (Applied-Biosystems) was used for quantitative real-time PCR (qRT-PCR) amplification with TaqMan assays and TaqMan fast advanced master mix (Applied Biosystems). Results were analysed with the standard ΔΔCt (cycle threshold) method; ΔΔCt= 2^(Ct of reference gene (β-Actin) – Ct of candidate gene). Primer sequences are listed in Supplemental Table 1. Genes with varying levels of fold-change were selected for qRT-PCR for a general validation of the microarray.

Results

Microarray data clustering

To investigate a possible role of fibroblast in the development of chronic inflammation in CRSwNP we performed whole-transcriptome microarray in cultured fibroblast from CRSwNP. To expose shifts in chromatin dynamics at different stages of the disease we used fibroblasts from nasal polyps (NPDF) and uncinate mucosa (UMDF) from patient with CRSwNP, and uncinate mucosa fibroblasts from healthy patients as controls. Our analysis identified 225 genes with differential expression among NPDF, UMDF and control samples (Figure 1A). Hierarchical clustering analysis and principal component analysis (PCA) revealed a stable gene signature in the NPDF samples that clustered together into a group segregated from control mucosae, whereas UMDF displayed an intermediate phenotype between that of control and NPDF subsets. Individual UMDF and NPDF samples from the same patient did not cluster together. All three subsets segregated along PC1 (35.5% variation) and PC6 (5.4% variation), displaying a transition from healthy mucosae to nasal polyps samples (Figure 1B). Among the top drivers genes we found *MAB21L1*, a cell-fate determinant, the NOTCH signaling ligand *JAG1*, *cKIT* tyrosine kinase and *LIMCH1*, which promotes the assembly of stress fibers [25] (Figure 1C).

Transcriptional switch in NPDF

We first focused on NPDF transcriptional profile and found 162 differentially expressed genes when compared to control samples: 101 were up-regulated and 61 were down-regulated in NPDF (Figure 1D; Supplemental Table 2). NPDF had increased levels of expression of extracellular adenosine signaling (such as *ENTPD1* (CD39), and *TXNIP*), a hypoxia-induced pathway that shift Th1 inflammatory response towards Th2 [26]. They also exhibited up-regulation of growth factors, such as *TGFB1*, *HGF* and *KITLG* also called Stem Cell Factor (SCF), the latter of which is a strong mediator of chronic Type-2 airway inflammation [27,28]. NPDF also displayed up-regulation of *ICAM1*, which mediates homing and activation of T cells by fibroblasts [29,30]. Notably, they exhibited broad up-regulation of ECM components and modulators (*Col11A1*, *TLL-1*, *VIT*, *LAMA4*, and *SULF2*). Among top differentially expressed genes we also found high expression levels of NOTCH (*JAG1*, *HES1*) and *KIT* (*KIT*, *KITLG*) signaling pathways signature genes. We confirmed high expression levels for *MAB21L1*, *ENTPD1* (CD39), *NFE2L3* and *KIT* by qRT-PCR to validate our study (Figure 1E). We also assayed *VEGFA* (relative values,1.05±0.22, n=5 control versus 1.39±0.43, n=5 UMDF versus 1.19±0.14, n=5 NPDF p>0.05) and *ACTA2* (relative values,1.08±0.24, n=5 control versus 1.51±0.14, n=5 UMDF versus 1.35±0.29, n=5 NPDF p>0.05), two genes not found in our microarray but previously reported as upregulated in NPDF [31–33]. Gene set enrichment analysis, using Hallmark curated database for canonical pathways, exposed a transcriptional switch in NPDF towards a pro-inflammatory gene expression profile. Notably, NPDF showed specific enrichment with several inflammatory signaling pathways, such as hypoxia, angiogenesis, inflammatory response, and coagulation (Figure 1F). Hallmark gene set enrichment analysis also identified enrichment in glycolysis

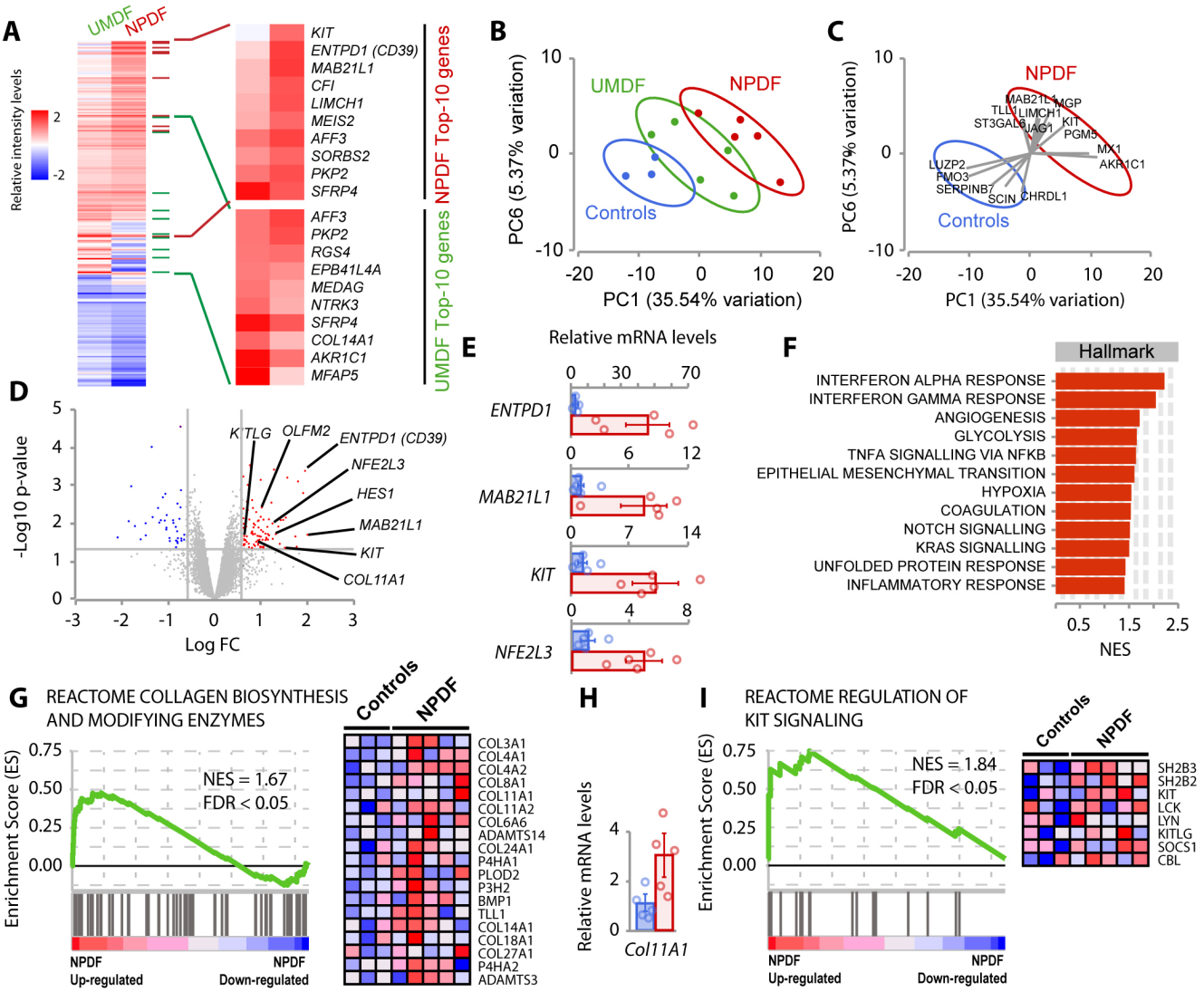

Figure 1. Transcriptome profiling of NPDF. A. Heat map showing the mean expression values of the 225 genes that separate UMDF and NPDF from control samples ordered by p-value. (Blue: down-regulation; Red: up-regulation). Top right corner panel depicts the top-10 more expressed genes in NPDF. Bottom right corner panel depicts top-10 more expressed genes in UMDF. B. Principal component analysis depicting the clustering of the samples along PC1 (35.5% variation) and PC6 (5.4% variation). C. Biplot of PC1 and PC6 with top 10% drivers genes. D. Volcano plot showing upregulated (red dots) and downregulated (blue dots) genes in NPDF compared to control samples. Lines indicate significance thresholds at –log10 p-value ≥ 1.3 and logFC ≤ -1.5 or ≥ 1.5. E. Relative expression levels of *ENTPD1*, *MAB21L1*, *KIT* and *NFE2L3* genes measured by qRT-PCR. Bars represent the mean ± S.E.M. in control (Blue) and NPDF (Red). F. Hallmark pathways analysed by GSEA in NPDF compared to control. Normalized enrichment score (NES) ≤ -1.4 or ≥ 1.4. G. Reactome enrichment analysis of collagen biosynthesis gene set. H. Relative expression levels of *COL11A1* measured by qRT-PCR. Bars represent the mean ± S.E.M. in control (blue) and NPDF (red). G. Reactome of regulation of KIT signalling enrichment analysis.

gene set, which could imply metabolic reprograming in NPDF, a hallmark of fibroblasts activation (Figure 1F). Moreover, *NFKB* and epithelial to mesenchymal transition gene sets were also enriched in NP fibroblasts, two pathways intimately connected to inflammation. NFKB is a key pro-inflammatory and pro-fibrotic transcription factor and a critical point of cross-talk between stress signals and metabolic reprograming [34,35]. NPDF were also enriched in interferon type I and type II responses (Figure 1F).

To further analyse NPDF transcriptional profile we investigated signaling pathway enrichment using Reactome curated gene set database [36]. Reactome analysis found enrichment with "collagen biosynthesis" terms in NPDF compared to controls (Figure 1G). We validated *COL11A1* by qRT-PCR to confirm these results (Figure 1H). Reactome enrichment analysis also exhibited enrichment in regulation of KIT signaling gene set at the top of the list (Figure 1I).

Overall, whole-transcriptome microarray data analysis exposed activation of a pro-inflammatory and pro-fibrotic gene expression signature in NPDF, when compared to healthy mucosa from control patients.

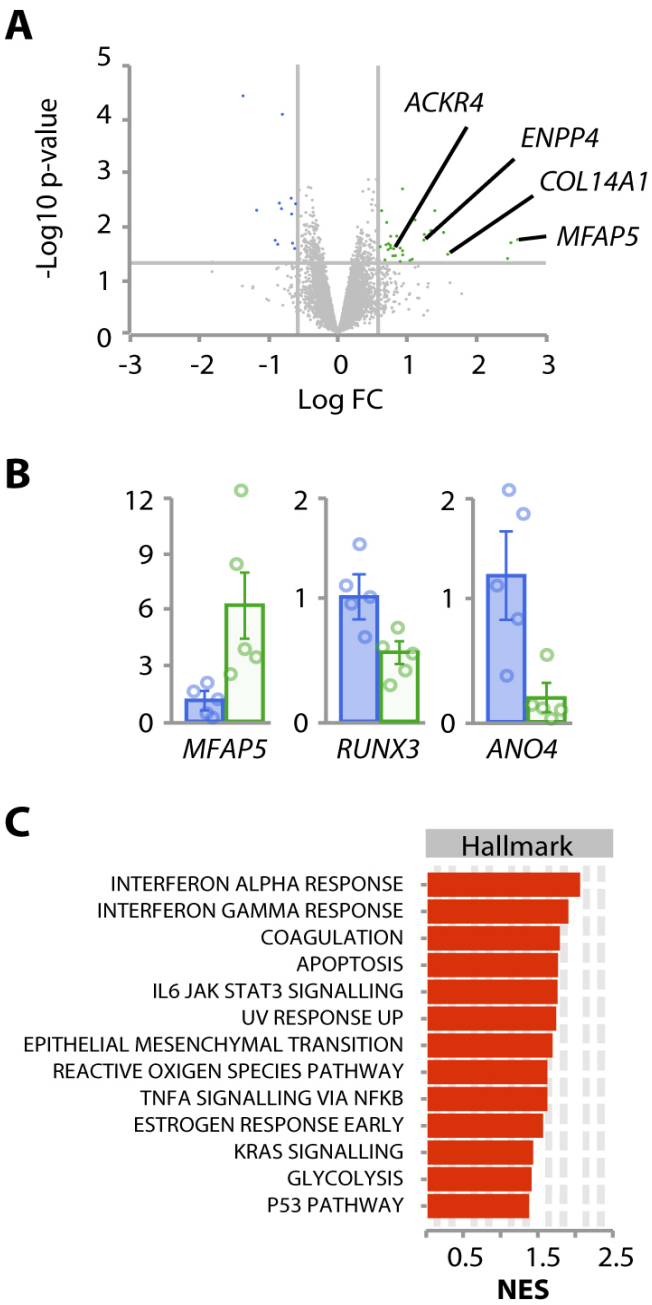

Figure 2. Up-regulation of a pro-inflammatory transcriptional profile in UMDF. A. Volcano plot showing up-regulated (green dots) and down-regulated (blue dots) genes in UM compared to control samples. Lines indicate significance thresholds at –log10 p-value ≥ 1.3 and logFC ≤ -1.5 or ≥ 1.5. B. Relative expression levels of *MFAP5*, *RUNX3* and *ANO4* measured by qRT-PCR. Bars represent the mean ± S.E.M. in control (blue) and UMDF (green). C. Hallmark gene set enrichment analysis in UMDF compared to control. Normalized enrichment score (NES) ≤-1.4 or ≥1.4.

UMDF transcriptional profile

We then focused on the transcriptional profile of UMDF to investigate whether they already displayed deregulated expression of inflammatory signals. We found 50 differentially expressed genes; 37 up-regulated and 13 down-regulated in UMDF when compared to controls (Figure 2A; Supplemental Table 3). In keeping with PCA and hieratical clustering data, UMDF gene signature intersected broadly with that of NPDF, though UMDF showed fewer differentially expressed genes (Figure 2A; Supplemental Table 2). UMDF exhibited up-regulation of ECM components and modulators (*SFRP4*, *SULF2*, *VIT* and *COL14A1*), and *MFAP5*, which encodes an ECM component proposed as cellular marker for collagen-producing fibroblasts in lower airways [37]. Notably, they also displayed high expression levels of the CCL19/CCL21 scavenger receptor *ACKR4*, which allows the egress of dendritic cells from inflamed peripheral tissue [38], and CXCL16, an inflammatory chemokine. We validated *MFAP5*, *RUNX3*, and *ANO4* by qRT-PCR (Figure 2B).

Hallmark enrichment analysis displayed enrichment with inflammatory terms such epithelial to mesenchymal transition, glycolysis, NFKB, coagulation and interferon type I and type II responses (Figure 2C), all of them also enriched in NPDF, as previously discussed. In addition to these seven common pathways, UMDF also exhibited enrichment with IL6 JAK STAT3 signaling gene set, and concomitant up-regulation of reactive oxygen species, apoptosis and p53 pathway gene sets (Figure 2C).

Taken together, these results indicate that fibroblasts from uncinate mucosa (UMDF) already feature pathological up-regulation of a pro-inflammatory transcriptional profile. Therefore, we next decided to compare NPDF and UMDF gene signatures to gain further insight into the development of pro-inflammatory status in nasal polyposis.

NPDF and UMDF expression profile comparison

Bilateral comparison of NPDF and UMDF identified 85 differentially expressed genes: 42 of them were up-regulated and 43 were down-regulated in NPDF (Figure 3A). NPDF displayed lower expression levels of mucosae-specific cell markers, such as *MFAP5* and *ACKR4*, and higher expression levels of *KIT*, *MAB21L1*, *COL11A1* and *ENTPD1* (CD39) when compared to UMDF (Figure 3A; Supplemental Table 4). We validated *ENTPD1*(CD39), *MAB21L1*, *MFAP5* and *ANO4* by qRT-PCR (Figure 3B). Principal component analysis segregated both groups along the PC1 (38.2% variation) axis, displaying a transition from uncinate mucosae to nasal polyps (Figure 3C). *BST2* [39], and *ST3GAL6* [40] genes associated to inflammatory-state in fibroblasts were identified as drivers for NPDF transcriptional signature, along with *TLL-1* (a ECM regulatory gene), *KIT* tyrosine kinase and MAB21L1 (Figure 3D). On the other hand, *MFAP5*, *OMD* and *FMO1* were confirmed as drivers of UMDF transcriptional signature (Figure 3D).

Hallmark gene set analysis displayed enrichment with inflammatory response, hypoxia, angiogenesis and glycolysis in NPDF when compared to UMDF, consistent with previous findings (Figure 3E). Notably, NPDF showed negative enrichment in p53 pathway, apoptosis and reactive oxygen species terms when

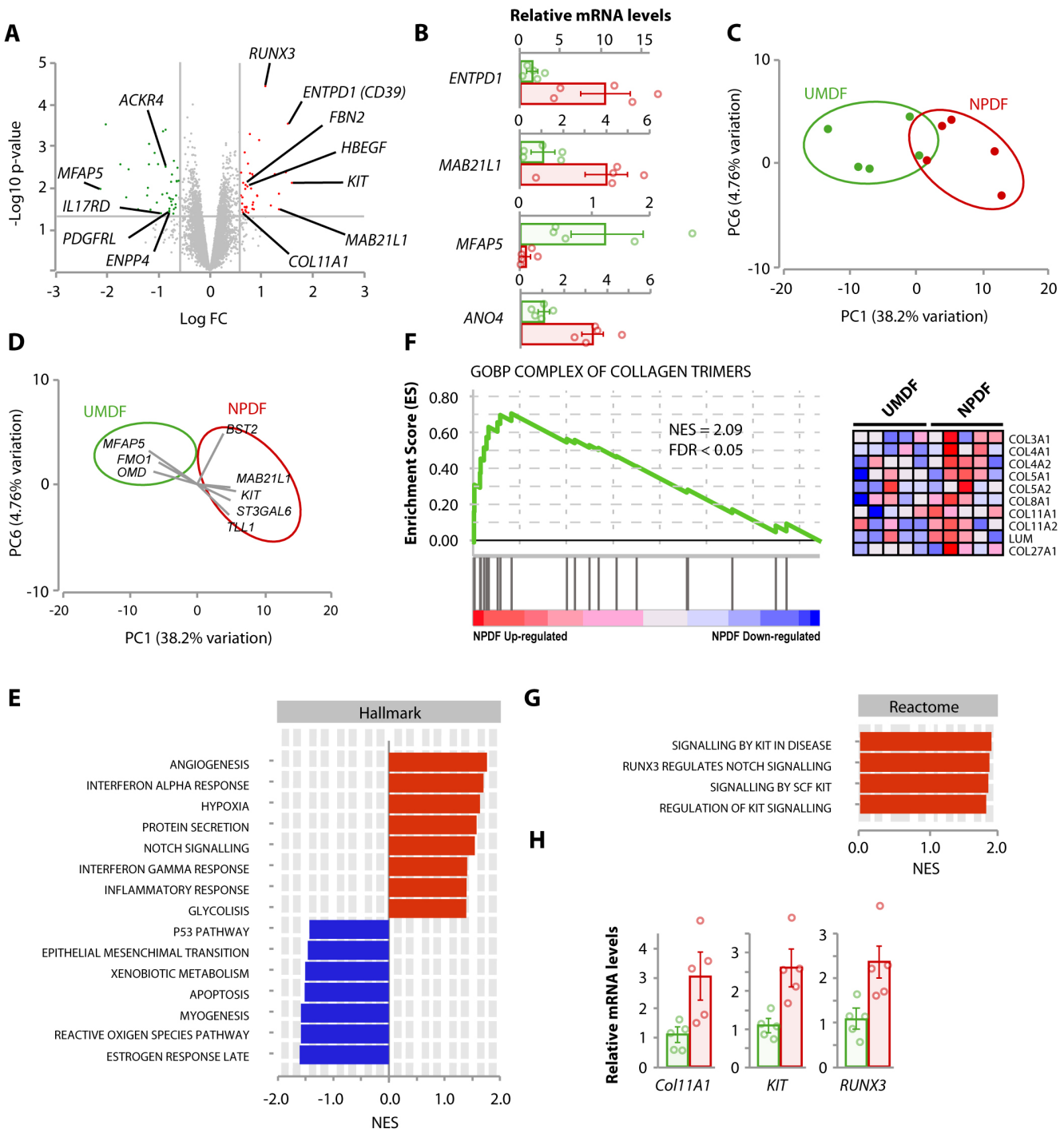

Figure 3. Differential gene expression comparison between NPDF and UMDF from CRSwNP patients. A. Volcano plot showing up-regulated (red dots) and down-regulated (green dots) genes in NPDF compared to UMDF. Lines indicate significance thresholds at –log10 p-value ≥ 1.3 and logFC ≤ -1.5 or ≥ 1.5. B. Relative expression levels of *ENTPD1*, *MAB21L1*, *MFAP5* and *ANO4* measured by qRT-PCR. Bars represent the mean ± S.E.M. in UMDF (green) and NPDF (red). C. Principal component analysis depicting the clustering of the samples along PC1 (38.2% variation) and PC6 (4.7% variation). D. Biplot of PC1 and PC6 with top 10% drivers genes. E. Hallmark gene set enrichment analysis in NPDF compared to UMDF. Normalized enrichment score (NES) ≤-1.4 or ≥1.4. F. Gene Ontology Biological Process (GOBP) of collagen trimmers gen set enrichment. G. Reactome enrichment analysis. H, Relative expression levels of *COL11A1*, *KIT* and *RUNX3* measured by qRT-PCR. Bars represent the mean ± S.E.M. in UMDF (green) and NPDF (red).

compared to UMDF (Figure 3E). GO terms enrichment analysis revealed enrichment in complex of collagen trimmers (Figure 3F), in agreement with the high levels of *COL11A1* and *FBN2* observed in the differential expression analysis (Figure 3A). Reactome enrichment analysis exhibited terms related to KIT and NOTCH signaling pathways at the top of the list (Figure 3G). We

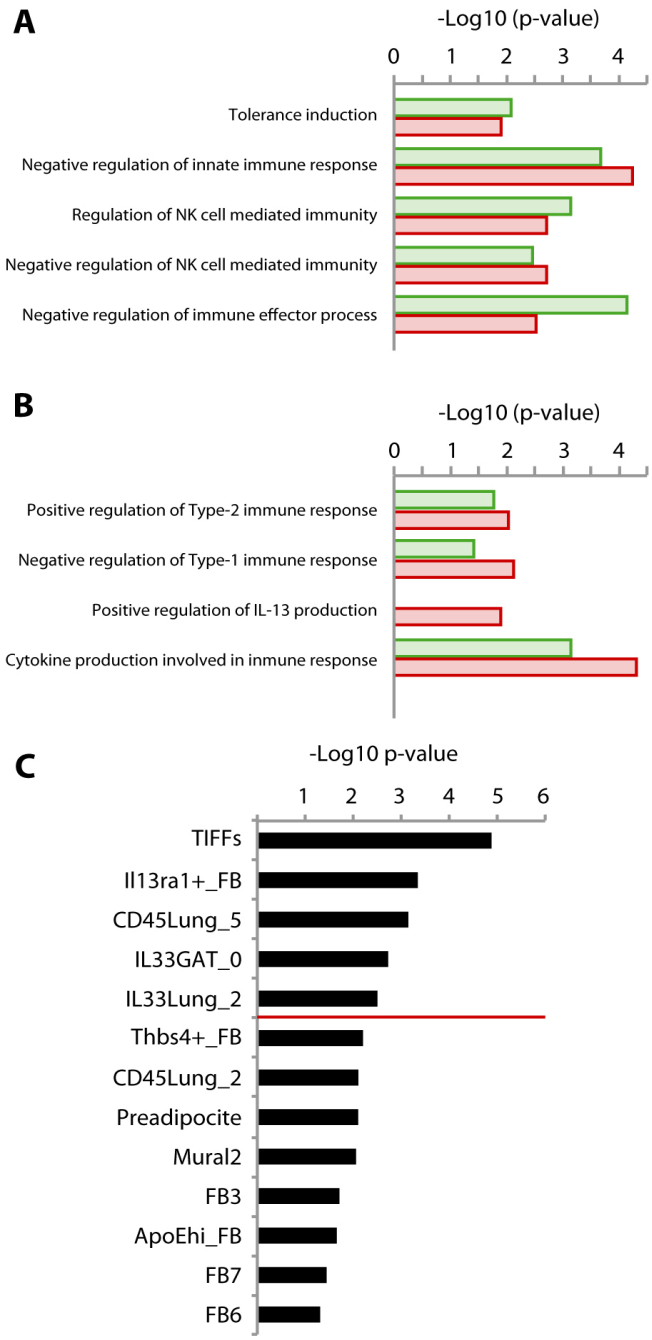

Figure 4. Fibroblast promoting Type-2 inflammatory response in CRSwNP. Selected Gene Ontology Biologicals Process enrichment analysis of immune response gene sets in UM and NP fibroblasts versus control samples. A, Gene sets related to resistance to cytotoxic immune attack. B, Gene sets related to modulation of immune response. (Green bars: UMDF; Red bars: NPDF). C. Gene Set Enrichment Analysis of gene signature markers in UMDF among cross-tissue mesenchymal cell-types. The red line separates type-2 inflammatory fibroblasts subsets from other cell-types. Data presented as -log10 (p-value).

confirmed by qRT-PCR specific up-regulation of *COL11A1*, *RUNX3* and *KIT* to further validate these results (Figure 3H).
Altogether, these results indicate that NPDF exhibit a more robust inflammatory response when compared to UMDF. Moreover, our analyses point to specific up-regulation of signaling pathways, such as KIT and NOTCH.

NPDF stimulate Type 2-promoting inflammatory response

Next, we explored whether fibroblasts might have a role in the modulation of the immune microenvironment in CRSwNP. Biological process enrichment analysis revealed that both UMDF and NPDF shared similar levels of enrichment with terms related to resistance to cytotoxic immune attack, such as tolerance induction and negative regulation of natural killer cell mediated immunity gene sets (Figure 4A) when compared to controls. Notably, UMDF and NPDF transcriptional signature exhibited good correlation with positive regulation of type-2 immune response and negative regulation of type-1 immune response gene sets (Figure 4B). Furthermore, although both UMDF and NPDF correlated with cytokine production involved in immune response, only NPDF exhibited high correlation with positive regulation of interleukin-13 production (Figure 4B), a mayor type-2 effector cytokine.
We then asked whether our fibroblasts show any transcriptional similarities with fibroblasts described in other pathologies. In particular, we were interested in a subset of fibroblasts called 'boundary fibroblasts', primed to support type-2 inflammatory response, and present in a wide range of tissues [41]. To test this hypothesis we took advantage of publicly available cross-tissue datasets of single-cell RNA sequencing of mesenchymal origin [3,8]. We calculated the enrichment of UMDF and NPDF markers in 62 mesenchymal cell-clusters from different tissues (Figure 4C). Surprisingly, UMDF displayed strong similarity to this subset of boundary fibroblasts, with all top five clusters corresponding to this cell type in skin, lung, and adipose tissues (Figure 4C). Thbs4+_FB represent a cluster of fibroblasts closely related to boundary fibroblasts transcriptional signature [3] that also shows correlation with UMDF signature (Figure 4C). On the other hand, NPDF did not show specific enrichment with this transcriptional signature.
Altogether, our results may indicate that these fibroblasts support type-2 inflammatory response in CRSwNP, and, in the case of UMDF, may be related to boundary fibroblasts. This subset of fibroblasts contributes to inflammation and tissue homeostasis in different organs [10], and has not been previously described in CRSwNP.

Discussion

Fibroblasts are cells at the crossroad of tissue homeostasis and inflammation, positioned to integrate damage signals and tissue-specific immune responses [1]. This study uncovers activation of a pro-inflammatory and pro-fibrotic transcriptional program in nasal polyps fibroblasts. Our work exposes a new source of sustained inflammatory signaling in a subset

of nasal polyps with otherwise unknown underlying cause of dysfunction. Furthermore, our results suggest that deregulated inflammatory signaling supports Type-2 inflammatory response in CRSwNP. Stress-activated fibroblasts that alter chromatin dynamics to support sustained tissue inflammation have been reported in a wide range of pathologies [6,7,42]. In the context of CRSwNP previous work identified epithelial cells as a source of inflammatory memory, and pointed to dysfunction in the fibroblasts compartment [12], yet this is the first comprehensive report of exacerbated fibroblasts activation in CRSwNP. Nevertheless, more work is needed to investigate the functional relevance of this shift in gene-expression patterns, as no protein levels were assayed, an important limitation of this study.

A growing body of evidence supports a major role for fibroblasts activation in tissue-specific inflammatory responses [2,3]. Upon activation fibroblasts increase secretion of growth factors, cytokines and ECM to promote immune response and tissue remodeling, processes that may trigger pathological inflammatory responses when deregulated [1]. In this work we have confirmed, (i) high expression levels of growth factors that modulate epithelial remodeling and proliferation, such as *HGF* and *TGFB1*, (ii) expression of cytokines that modulate immune microenvironment in CRSwNP, namely, CXCL16 and *ACKR4* [38], or *KITLG* [28], and adenosine extracellular signaling [43], and (iii) CRSwNP and polyps fibroblasts present broad up-regulation of ECM components and modulators. Moreover, CRSwNP fibroblasts pointed to a pro-inflammatory molecular signature concordant with a metabolic shift towards normoxic glycolysis, which has been proposed as a hallmark of fibroblasts activation [44] in other inflammatory diseases [2,45]. Alternatively, tissue-resident fibroblasts can also support sustained inflammatory response by increasing their life span [46]. Interestingly, polyps fibroblasts showed resistance to cytotoxic attack and reduced apoptotic signaling, which may account for extended survival of these inflammatory fibroblasts, and arguably sustain inflammation for longer periods in vivo [47]. Altogether, cumulatively these results indicate that CRSwNP correspond to activated or primed fibroblasts that may exaggeratedly respond to immune challenges in vivo.

Our work also highlights activated molecular pathways, which might have an impact in the development of inflammatory status in CRSwNP fibroblasts. In particular our data suggest that cKit tyrosine kinase and NOTCH could be important factors in the emergence or maintenance of NPDF phenotype. For future studies, we aim to elucidate the contribution of these pathways to NPDF phenotype.

Our results indicate that CRSwNP fibroblasts may have the capacity to modulate CRSwNP immune microenvironment. On one hand, UMDF expressed high levels of cytokines that regulate leucocytes and dendritic cells traffic, such as CXCL16 and *ACKR4* [38]. On the other hand, NPDF showed increased capacity to interact with immune cells via ICAM-1 [29,30]. Of note, our results strongly suggest that CRSwNP and polyps fibroblasts express activation of a pro-inflammatory transcriptional program, supporting a type-2 inflammatory response. We have found higher expression levels of extracellular adenosine signaling and *KITLG* in NPDF. More experiments are needed to elucidate the in vivo importance of these signals. Nevertheless, as discussed before, fibroblasts interact directly with leucocytes to integrate danger signals and immune effector responses [48], and therefore, modest increases in cytokine release may have a huge impact in the modulation of the immune responses.

Of note, our results also indicate that UMDF share robust similarity to boundary fibroblasts core transcriptional signature. This is a subset described in many tissues [41] that present varying combinations of cell markers [3]. These boundary fibroblasts are primed to support a type-2 inflammatory response, and are well documented to cause exacerbated inflammatory responses when deregulated [10]. These results open new perspectives in the study of CRSwNP inflammatory signaling and raise questions regarding the role of fibroblasts in the emergence of CRSwNP chronic inflammation. Moreover, direct interaction of this subset of fibroblasts, and Th2-cells has been recently revealed in certain niches along the body axis [8,49,50]. Additionally, discrete subsets of ILC2-interacting fibroblasts have also been identified as promoters of type-2 immune responses in lungs, perivascular niches, adipose tissue and pancreas [8,49,50], which could indicate a conserved mechanism of cross-tissue type-2 immune response regulation. Hence, for future directions we aim to further investigate the functional relevance of these signaling pathways. Additionally, we intend to investigate the relationship of CRSwNP fibroblasts and boundary fibroblasts, whether niche-specific interactions could also take place in upper airway, and to elucidate the precise contribution of these interactions to the CRSwNP pathophysiology.

Authorship contribution

CPG, JLMB, RML and SSG: designed the study. CPG, JLMB, RML and SSG: designed the experiments. JMPG, CPG and JLMB: performed experiments. JACV, JMPG, JLMB and CPG: analysed the data. AC, OP, GA, JMMS, RML, SSG, CPG, VSM and JLMB: participated in the discussion of data. RML, CPG and SSG: supervised the project. AC, OP, GA, JMMS, VSM, RML and SSG: participated in the critical revision of the manuscript. CPG, RML and JLMB: wrote the manuscript.

Acknowledgement

Authors want to acknowledge the patients for their participation in this study, Dr. Tarik Smani for the loan of equipment and the "Consejería de Salud y Familias, Junta de Andalucía" for the funding. We also want to thank the Genomics and Research Support Facilities of the Institute of Biomedicine of Seville, especially to Francisco J. Morón Civanto and Raquel Gómez Díaz for their

technical help in this work.

Conflict of interest

The authors declare no conflict of interest.

Funding

This work was supported by Grant PI-0212-2017, PIGE-0367-2019 and RH-0048-2021 of the "Consejería de Salud y Familias, Junta de Andalucía" Spain.

References

1. Nowarski R, Jackson R, Flavell RA The stromal intervention: regulation of immunity and inflammation at the epithelial-mesenchymal barrier. Cell 2017;168(3):362–75.
2. Friščić J, Böttcher M, Reinwald C, et al. The complement system drives local inflammatory tissue priming by metabolic reprogramming of synovial fibroblasts Immunity 2021;54(5):1002-1021e10.
3. Boothby IC, Kinet MJ, Boda DP, et al. Early-life inflammation primes a T helper 2 cell–fibroblast niche in skin. Nature. 2021 Nov;599(7886):667-672.
4. Crowley T, Buckley CD, Clark AR. Stroma: the forgotten cells of innate immune memory. Clin Exp Immunol. 2018;193(1):24–36.
5. Rockey DC, Bell PD, Hill JA. Fibrosis — A common pathway to organ injury and failure. N Engl J Med. 2015;372(12):1138–49.
6. Alexanian M, Przytycki PF, Micheletti R, et al. A transcriptional switch governs fibroblast activation in heart disease. Nature. 2021;595(7867):438–43.
7. Shin JY, Beckett JD, Bagirzadeh R, et al. Epigenetic activation and memory at a TGFB2 enhancer in systemic sclerosis. Sci Transl Med. 2019;11(497).
8. Dahlgren MW, Jones SW, Cautivo KM, et al. Adventitial stromal cells define group 2 innate lymphoid cell tissue niches. Immunity. 2019;50(3):707-722.e6.
9. Buechler MB, Turley SJ. A short field guide to fibroblast function in immunity. Semin Immunol. 2018;35:48–58.
10. Dahlgren MW, Molofsky AB. Adventitial cuffs: regional hubs for tissue immunity. Trends Immunol. 2019;40(10):877–87.
11. Schleimer RP. Immunopathogenesis of chronic rhinosinusitis and nasal polyposis. Annu Rev Pathol Mech Dis. 2017;12(1):331–57.
12. Ordovas-Montanes J, Dwyer DF, Nyquist SK, et al. Allergic inflammatory memory in human respiratory epithelial progenitor cells. Nature. 2018;560(7720):649-654.
13. Gevaert P, Van Bruaene N, Cattaert T, et al. Mepolizumab, a humanized anti–IL-5 mAb, as a treatment option for severe nasal polyposis. J Allergy Clin Immunol. 2011;128(5):989-995.e8.
14. Gevaert P, Calus L, Van Zele T, et al. Omalizumab is effective in allergic and nonallergic patients with nasal polyps and asthma. J Allergy Clin Immunol. 2013;131(1):110-116.e1.
15. Bachert C, Mannent L, Naclerio RM, et al. Effect of subcutaneous dupilumab on nasal polyp burden in patients with chronic sinusitis and nasal polyposis. JAMA. 2016;315(5):469.
16. Hsu J, Avila PC, Kern RC, Hayes MG, Schleimer RP, Pinto JM. Genetics of chronic rhinosinusitis: State of the field and directions forward. J Allergy Clin Immunol. 2013;131(4):977-993.e5.
17. Mfuna-Endam L, Zhang Y, Desrosiers MY. Genetics of rhinosinusitis. Curr Allergy Asthma Rep. 2011;11(3):236–46.
18. Fokkens WJ, Lund VJ, Hopkins C, et al. Executive summary of EPOS 2020 including integrated care pathways. Rhinology. 2020;58(2):82–111.
19. Lund V, Kennedy D. Staging for rhinosinusitis. Otolaryngol - Head Neck Surg. 1997;117(3):S35–40.
20. Executive Committee GEMA 2009. GEMA 2009 (Spanish guideline on the management of asthma). J Investig Allergol Clin Immunol. 2010;20 Suppl 1:1–59.
21. Bousquet J, Khaltaev N, Cruz AA, et al. Allergic rhinitis and its impact on asthma (ARIA) 2008*. Allergy. 2008;63:8–160.
22. Moon Y-M, Kang HJ, Cho J-S, Park I-H, Lee H-M. Nox4 mediates hypoxia-stimulated myofibroblast differentiation in nasal polyp-derived fibroblasts. Int Arch Allergy Immunol. 2012;159(4):399–409.
23. Rodríguez-Núñez P, Romero-Pérez L, Amaral AT, et al. Hippo pathway effectors YAP1/TAZ induce an EWS–FLI1-opposing gene signature and associate with disease progression in Ewing sarcoma. J Pathol. 2020;250(4):374–86.
24. Subramanian A, Tamayo P, Mootha VK, et al. Gene set enrichment analysis: A knowledge-based approach for interpreting genome-wide expression profiles. Proc Natl Acad Sci. 2005;102(43):15545–50.
25. Lin Y-H, Zhen Y-Y, Chien K-Y, et al. LIMCH1 regulates nonmuscle myosin-II activity and suppresses cell migration. Mol Biol Cell. 2017;28(8):1054–65.
26. Eltzschig HK, Sitkovsky M V., Robson SC. Purinergic signaling during inflammation. N Engl J Med. 2012 Dec 13;367(24):2322-33.
27. Lukacs NW. Role of chemokines in the pathogenesis of asthma. Nat Rev Immunol. 2001;1(2):108–16.
28. Fonseca W, Rasky AJ, Ptaschinski C, et al. Group 2 innate lymphoid cells (ILC2) are regulated by stem cell factor during chronic asthmatic disease. Mucosal Immunol. 2019;12(2):445–56.
29. Walling BL, Kim M. LFA-1 in T cell migration and differentiation. Front Immunol. 2018;9,952.
30. Verma NK, Kelleher D. Not just an adhesion molecule: LFA-1 contact tunes the T lymphocyte program. J Immunol. 2017;199(4):1213–21.
31. Wittekindt C, Hess A, Bloch W, Sultanie S, Michel O. Immunohistochemical expression of VEGF and VEGF receptors in nasal polyps as compared to normal turbinate mucosa. Eur Arch Oto-Rhino-Laryngology. 2002;259(6):294–8.
32. Park H-H, Park I-H, Cho J-S, Lee Y-M, Lee H-M. The effect of macrolides on myofibroblast differentiation and collagen production in nasal polyp–derived fibroblasts. Am J Rhinol Allergy. 2010;24(5):348–53.
33. Lin S-K, Shun C-T, Kok S-H, Wang C-C, Hsiao T-Y, Liu C-M. Hypoxia-stimulated vascular endothelial growth factor production in human nasal polyp fibroblasts. Arch Otolaryngol Neck Surg. 2008;134(5):522.
34. Celebrating 25 years of NF-κB. Nat Immunol. 2011;12(8):681–681.
35. Mauro C, Leow SC, Anso E, et al. NF-κB controls energy homeostasis and metabolic adaptation by upregulating mitochondrial respiration. Nat Cell Biol. 2011;13(10):1272–9.
36. Jassal B, Matthews L, Viteri G, et al. The reactome pathway knowledgebase. Nucleic Acids Res. 2020;48(D1):D498-D503.
37. Valenzi E, Bulik M, Tabib T, et al. Single-cell analysis reveals fibroblast heterogeneity and myofibroblasts in systemic sclerosis-associated interstitial lung disease. Ann Rheum Dis. 2019;78(10):1379–87.
38. Bastow CR, Bunting MD, Kara EE, et al. Scavenging of soluble and immobilized CCL21 by ACKR4 regulates peripheral dendritic cell emigration. Proc Natl Acad Sci. 2021;118(17):e2025763118.
39. Boyd DF, Allen EK, Randolph AG, et al. Exuberant fibroblast activity compromises lung function via ADAMTS4. Nature. 2020;587(7834):466–71.
40. Wang Y, Khan A, Antonopoulos A, et al. Loss of α2-6 sialylation promotes the transformation of synovial fibroblasts into a pro-inflammatory phenotype in arthritis. Nat Commun. 2021;12(1):2343.
41. Buechler MB, Pradhan RN, Krishnamurty AT, et al. Cross-tissue organization of the fibroblast lineage. Nature. 2021;593(7860):575–9.
42. Croft AP, Campos J, Jansen K, et al. Distinct fibroblast subsets drive inflammation and damage in arthritis. Nature. 2019;570(7760):246–51.
43. Sitkovsky M, Lukashev D. Regulation of immune cells by local-tissue oxygen tension: HIF1α and adenosine receptors. Nat Rev Immunol. 2005;5(9):712–21.
44. Kozlov AM, Lone A, Betts DH, Cumming RC. Lactate preconditioning promotes a HIF-1α-mediated metabolic shift from OXPHOS to

glycolysis in normal human diploid fibroblasts. Sci Rep. 2020;10(1):8388.
45. Henderson J, Duffy L, Stratton R, Ford D, O'Reilly S. Metabolic reprogramming of glycolysis and glutamine metabolism are key events in myofibroblast transition in systemic sclerosis pathogenesis. J Cell Mol Med. 2020;24(23):14026–38.
46. Jun J-I, Lau LF. Resolution of organ fibrosis. J Clin Invest. 2018;128(1):97–107.
47. Huang SK, Scruggs AM, Donaghy J, et al. Histone modifications are responsible for decreased Fas expression and apoptosis resistance in fibrotic lung fibroblasts. Cell Death Dis. 2013;4(5):e621–e621.
48. Davidson S, Coles M, Thomas T, et al. Fibroblasts as immune regulators in infection, inflammation and cancer. Nat Rev Immunol. 2021;21(11):704–17.
49. Rana BMJ, Jou E, Barlow JL, et al. A stromal cell niche sustains ILC2-mediated type-2 conditioning in adipose tissue. J Exp Med. 2019;216(9):1999–2009.
50. Dalmas E, Lehmann FM, Dror E, et al. Interleukin-33-activated islet-resident innate lymphoid cells promote insulin secretion through myeloid cell retinoic acid production. Immunity. 2017;47(5):928-942.e7.

Cristina Porras-González, PhD
Rhinology Unit
Department of Otolaryngology
Head and Neck Surgery
Virgen Macarena University Hospital
FISEVI.
Seville
Spain

Tel: +34 666253722
E-mail: cristinaporras-ibis@us.es"

Ramón Moreno-Luna, MD, PhD
Advisory Board of European Rhinology Society
Rhinology Unit
Department of Otolaryngology
Hospital Universitario Virgen de la Macarena
Avda. Doctor Fedriani 3
E-41071 Seville
Spain

Tel : 034 661818838
E-mail : ramoluorl@gmail.com

This manuscript contains online supplementary material

SUPPLEMENTARY MATERIAL

Supplementary Table 1. List of primer sequences.

Gene	Primer
MAB21L1	Hs00366575_s1
ENTPD1	Hs00969559_m1
KIT	Hs00174029_m1
COL11A1	Hs01097664_m1
ANO4	Hs01128244_m1
NFE2L3	Hs00852569_m1
RUNX3	Hs00231709_m1
MFAP5	Hs00969608_g1
ACTA2	Hs00426835_g1
VEGFA	Hs00900055_m1
ACTB	Hs99999903_m1

Supplementary Table 2. List of differential expression genes NPDF vs Controls.

Entrez_ gene_id	logFC	FC	P.Value	Symbol	Alias	Gene_name
4081	2.00	3.99	0.02	MAB21L1	CAGR1	mab-21 like 1
953	1.94	3.85	0.00	ENTPD1	ATPDase	ectonucleoside triphosphate diphosphohydrolase 1
3899	1.91	3.75	0.00	AFF3	LAF4	AF4/FMR2 family member 3
5318	1.80	3.47	0.00	PKP2	ARVD9	plakophilin 2
22998	1.77	3.40	0.04	LIMCH1	LIMCH1A	LIM and calponin homology domains 1
3426	1.74	3.34	0.02	CFI	AHUS3	complement factor I
8470	1.57	2.96	0.00	SORBS2	ARGBP2	sorbin and SH3 domain containing 2
4212	1.53	2.89	0.01	MEIS2	CPCMR	Meis homeobox 2
3815	1.51	2.85	0.04	KIT	C-Kit	KIT proto-oncogene. receptor tyrosine kinase
5999	1.47	2.78	0.01	RGS4	RGP4	regulator of G protein signaling 4
145258	1.42	2.68	0.01	GSC	SAMS	goosecoid homeobox
10964	1.40	2.64	0.03	IFI44L	C1orf29	interferon induced protein 44 like
8854	1.37	2.59	0.01	ALDH1A2	RALDH(II)	aldehyde dehydrogenase 1 family member A2
3280	1.32	2.49	0.02	HES1	HES-1	hes family bHLH transcription factor 1
28951	1.28	2.43	0.00	TRIB2	C5FW	tribbles pseudokinase 2
56892	1.25	2.38	0.03	TCIM	C8orf4	transcriptional and immune response regulator
9603	1.24	2.37	0.01	NFE2L3	NRF3	nuclear factor. erythroid 2 like 3
7045	1.22	2.33	0.00	TGFBI	BIGH3	transforming growth factor beta induced
81849	1.17	2.25	0.02	ST6GALNAC5	SIAT7-E	ST6 N-acetylgalactosaminide alpha-2.6-sialyltransferase 5
4599	1.17	2.25	0.01	MX1	IFI-78K	MX dynamin like GTPase 1
3875	1.15	2.22	0.02	KRT18	CK-18	keratin 18
64097	1.15	2.21	0.03	EPB41L4A	EPB41L4	erythrocyte membrane protein band 4.1 like 4A
128553	1.13	2.19	0.01	TSHZ2	C20orf17	teashirt zinc finger homeobox 2
100131187	1.11	2.17	0.03	TSTD1	KAT	thiosulfate sulfurtransferase like domain containing 1
8972	1.11	2.16	0.02	MGAM	MG	maltase-glucoamylase
10085	1.10	2.14	0.02	EDIL3	DEL1	EGF like repeats and discoidin domains 3

Entrez_ gene_id	logFC	FC	P.Value	Symbol	Alias	Gene_name
23284	1.09	2.14	0.03	ADGRL3	CIRL3	adhesion G protein-coupled receptor L3
4741	1.05	2.07	0.04	NEFM	NEF3	neurofilament medium
8835	1.05	2.07	0.01	SOCS2	CIS2	suppressor of cytokine signaling 2
8490	1.05	2.07	0.04	RGS5	MST092	regulator of G protein signaling 5
10125	1.05	2.07	0.05	RASGRP1	CALDAG-GEFI	RAS guanyl releasing protein 1
4147	1.04	2.06	0.02	MATN2	MATN2	matrilin 2
182	1.03	2.05	0.04	JAG1	AGS	jagged canonical Notch ligand 1
121506	1.03	2.04	0.03	ERP27	C12orf46	endoplasmic reticulum protein 27
93145	1.01	2.02	0.00	OLFM2	NOE2	olfactomedin 2
100507421	1.00	2.00	0.01	TMEM178B	TMEM178B	transmembrane protein 178B
56033	1.00	1.99	0.04	BARX1	BARX1	BARX homeobox 1
23231	0.99	1.99	0.02	SEL1L3	Sel-1L3	SEL1L family member 3
27286	0.99	1.99	0.00	SRPX2	BPP	sushi repeat containing protein X-linked 2
50863	0.99	1.99	0.01	NTM	CEPU-1	neurotrimin
54873	0.99	1.98	0.05	PALMD	C1orf11	palmdelphin
1909	0.99	1.98	0.04	EDNRA	ET-A	endothelin receptor type A
26034	0.98	1.97	0.04	IPCEF1	PIP3-E	interaction protein for cytohesin exchange factors 1
55786	0.96	1.95	0.03	ZNF415	Pact	zinc finger protein 415
3965	0.96	1.94	0.02	LGALS9	HUAT	galectin 9
8436	0.95	1.93	0.01	CAVIN2	PS-p68	caveolae associated protein 2
397	0.95	1.93	0.05	ARHGDIB	D4	Rho GDP dissociation inhibitor beta
54762	0.94	1.92	0.01	GRAMD1C	GRAMD1C	GRAM domain containing 1C
57608	0.94	1.92	0.03	JCAD	KIAA1462	junctional cadherin 5 associated
23043	0.93	1.91	0.04	TNIK	MRT54	TRAF2 and NCK interacting kinase
55959	0.93	1.91	0.01	SULF2	HSULF-2	sulfatase 2
1301	0.93	1.90	0.03	COL11A1	CO11A1	collagen type XI alpha 1 chain
5212	0.92	1.89	0.02	VIT	VIT1	vitrin
152330	0.90	1.86	0.03	CNTN4	AXCAM	contactin 4
26289	0.89	1.86	0.01	AK5	AK6	adenylate kinase 5
286183	0.87	1.83	0.02	NKAIN3	FAM77D	sodium/potassium transporting ATPase interacting 3
9076	0.87	1.82	0.01	CLDN1	CLD1	claudin 1
401089	0.87	1.82	0.04	FOXL2NB	C3orf72	FOXL2 neighbor
8612	0.84	1.80	0.04	PLPP2	LPP2	phospholipid phosphatase 2
221687	0.84	1.79	0.01	RNF182	RNF182	ring finger protein 182
1138	0.84	1.79	0.01	CHRNA5	LNCR2	cholinergic receptor nicotinic alpha 5 subunit
23705	0.82	1.77	0.02	CADM1	BL2	cell adhesion molecule 1
5738	0.82	1.77	0.00	PTGFRN	CD315	prostaglandin F2 receptor inhibitor
23460	0.81	1.76	0.02	ABCA6	EST155051	ATP binding cassette subfamily A member 6
10659	0.81	1.75	0.02	CELF2	BRUNOL3	CUGBP Elav-like family member 2
107987150	0.81	1.75	0.00	LOC107987150	LOC107987150	uncharacterized LOC107987150
64798	0.81	1.75	0.04	DEPTOR	DEP.6	DEP domain containing MTOR interacting protein
1363	0.79	1.73	0.02	CPE	CPH	carboxypeptidase E
10653	0.78	1.72	0.00	SPINT2	DIAR3	serine peptidase inhibitor. Kunitz type 2
1124	0.76	1.70	0.00	CHN2	ARHGAP3	chimerin 2
220441	0.75	1.68	0.01	RNF152	RNF152	ring finger protein 152
5734	0.74	1.67	0.04	PTGER4	EP4	prostaglandin E receptor 4

Entrez_ gene_id	logFC	FC	P.Value	Symbol	Alias	Gene_name
8614	0.73	1.66	0.03	STC2	STC-2	stanniocalcin 2
9843	0.72	1.64	0.00	HEPH	CPL	hephaestin
51477	0.71	1.64	0.00	ISYNA1	INO1	inositol-3-phosphate synthase 1
3105	0.69	1.62	0.00	HLA-A	HLAA	major histocompatibility complex. class I. A
3708	0.69	1.62	0.02	ITPR1	ACV	inositol 1.4.5-trisphosphate receptor type 1
390067	0.69	1.61	0.03	OR52H1	OR11-41	olfactory receptor family 52 subfamily H member 1
120065	0.68	1.60	0.01	OR5P2	JCG3	olfactory receptor family 5 subfamily P member 2
3082	0.66	1.58	0.03	HGF	DFNB39	hepatocyte growth factor
106707243	0.65	1.57	0.04	PRH1-TAS2R14	PRH1-TAS2R14	PRH1-TAS2R14 readthrough
3383	0.65	1.56	0.03	ICAM1	BB2	intercellular adhesion molecule 1
3764	0.64	1.56	0.04	KCNJ8	KIR6.1	potassium inwardly rectifying channel subfamily J member 8
4254	0.64	1.56	0.02	KITLG	DCUA	KIT ligand
10846	0.63	1.55	0.03	PDE10A	ADSD2	phosphodiesterase 10A
2296	0.63	1.55	0.05	FOXC1	ARA	forkhead box C1
5069	0.63	1.55	0.04	PAPPA	ASBABP2	pappalysin 1
3910	0.63	1.55	0.01	LAMA4	CMD1JJ	laminin subunit alpha 4
79956	0.63	1.55	0.04	ERMP1	FXNA	endoplasmic reticulum metallopeptidase 1
2675	0.62	1.54	0.01	GFRA2	GDNFRB	GDNF family receptor alpha 2
79858	0.62	1.54	0.00	NEK11	NEK11	NIMA related kinase 11
10628	0.62	1.54	0.01	TXNIP	ARRDC6	thioredoxin interacting protein
3106	0.62	1.53	0.00	HLA-B	AS	major histocompatibility complex. class I. B
29063	0.60	1.52	0.00	ZCCHC4	HSPC052	zinc finger CCHC-type containing 4
27152	0.60	1.52	0.01	INTU	CPLANE4	inturned planar cell polarity protein
23475	0.60	1.51	0.03	QPRT	HEL-S-90n	quinolinate phosphoribosyltransferase
166647	0.60	1.51	0.02	ADGRA3	GPR125	adhesion G protein-coupled receptor A3
9056	0.60	1.51	0.01	SLC7A7	LAT3	solute carrier family 7 member 7
7694	0.59	1.50	0.01	ZNF135	ZNF61	zinc finger protein 135
80127	0.59	1.50	0.00	BBOF1	C14orf45	basal body orientation factor 1
8029	0.58	1.50	0.04	CUBN	IFCR	cubilin
101926926	-0.58	-1.50	0.00	RDH10-AS1	RDH10-AS1	RDH10 antisense RNA 1
26952	-0.58	-1.50	0.00	SMR3A	P-B1	submaxillary gland androgen regulated protein 3A
63898	-0.58	-1.50	0.04	SH2D4A	PPP1R38	SH2 domain containing 4A
90139	-0.58	-1.50	0.01	TSPAN18	TSPAN	tetraspanin 18
11240	-0.58	-1.50	0.00	PADI2	PAD-H19	peptidyl arginine deiminase 2
121601	-0.59	-1.50	0.02	ANO4	TMEM16D	anoctamin 4
1366	-0.59	-1.51	0.01	CLDN7	CEPTRL2	claudin 7
23119	-0.59	-1.51	0.05	HIC2	HRG22	HIC ZBTB transcriptional repressor 2
338322	-0.59	-1.51	0.02	NLRP10	CLR11.1	NLR family pyrin domain containing 10
342538	-0.60	-1.51	0.02	NACA2	ANAC	nascent polypeptide associated complex subunit alpha 2
221458	-0.60	-1.51	0.00	KIF6	C6orf102	kinesin family member 6
4233	-0.60	-1.52	0.02	MET	AUTS9	MET proto-oncogene. receptor tyrosine kinase
822	-0.60	-1.52	0.03	CAPG	AFCP	capping actin protein. gelsolin like
290	-0.60	-1.52	0.05	ANPEP	APN	alanyl aminopeptidase. membrane
60370	-0.60	-1.52	0.01	AVPI1	PP5395	arginine vasopressin induced 1
219970	-0.60	-1.52	0.00	GLYATL2	BXMAS2-10	glycine-N-acyltransferase like 2
221749	-0.61	-1.52	0.01	PXDC1	C6orf145	PX domain containing 1

Entrez_ gene_id	logFC	FC	P.Value	Symbol	Alias	Gene_name
729220	-0.61	-1.53	0.05	FLJ45513	FLJ45513	uncharacterized LOC729220
5733	-0.65	-1.57	0.02	PTGER3	EP3	prostaglandin E receptor 3
6474	-0.66	-1.58	0.03	SHOX2	OG12	short stature homeobox 2
154141	-0.70	-1.62	0.05	MBOAT1	LPEAT1	membrane bound O-acyltransferase domain containing 1
22943	-0.70	-1.63	0.05	DKK1	DKK-1	dickkopf WNT signaling pathway inhibitor 1
85462	-0.71	-1.64	0.03	FHDC1	INF1	FH2 domain containing 1
10516	-0.72	-1.64	0.02	FBLN5	ADCL2	fibulin 5
8323	-0.72	-1.65	0.00	FZD6	FZ-6	frizzled class receptor 6
8492	-0.73	-1.66	0.00	PRSS12	BSSP-3	serine protease 12
5167	-0.73	-1.66	0.00	ENPP1	ARHR2	ectonucleotide pyrophosphatase/phosphodiesterase 1
84302	-0.75	-1.69	0.01	PGAP4	C9orf125	post-GPI attachment to proteins GalNAc transferase 4
8671	-0.79	-1.73	0.02	SLC4A4	HNBC1	solute carrier family 4 member 4
256691	-0.80	-1.74	0.03	MAMDC2	MAMDC2	MAM domain containing 2
3696	-0.80	-1.74	0.00	ITGB8	ITGB8	integrin subunit beta 8
84189	-0.80	-1.74	0.03	SLITRK6	DFNMYP	SLIT and NTRK like family member 6
117581	-0.80	-1.75	0.02	TWIST2	AMS	twist family bHLH transcription factor 2
54829	-0.83	-1.77	0.04	ASPN	OS3	asporin
4856	-0.83	-1.78	0.03	CCN3	IBP-9	cellular communication network factor 3
23314	-0.83	-1.78	0.01	SATB2	GLSS	SATB homeobox 2
9365	-0.86	-1.82	0.05	KL	HFTC3	klotho
54947	-0.88	-1.85	0.01	LPCAT2	AGPAT11	lysophosphatidylcholine acyltransferase 2
57604	-0.89	-1.85	0.01	TRMT9B	C8orf79	tRNA methyltransferase 9B (putative)
1382	-0.92	-1.90	0.05	CRABP2	CRABP-II	cellular retinoic acid binding protein 2
9953	-0.96	-1.95	0.03	HS3ST3B1	3-OST-3B	heparan sulfate-glucosamine 3-sulfotransferase 3B1
4237	-0.96	-1.95	0.05	MFAP2	MAGP	microfibril associated protein 2
113146	-0.97	-1.96	0.02	AHNAK2	C14orf78	AHNAK nucleoprotein 2
55089	-1.03	-2.04	0.01	SLC38A4	ATA3	solute carrier family 38 member 4
374462	-1.03	-2.05	0.01	PTPRQ	DFNA73	protein tyrosine phosphatase receptor type Q
22871	-1.04	-2.05	0.01	NLGN1	NL1	neuroligin 1
2702	-1.06	-2.08	0.00	GJA5	ATFB11	gap junction protein alpha 5
639	-1.07	-2.10	0.01	PRDM1	BLIMP1	PR/SET domain 1
7164	-1.11	-2.16	0.00	TPD52L1	D53	TPD52 like 1
92949	-1.15	-2.22	0.01	ADAMTSL1	ADAMTSL-1	ADAMTS like 1
389558	-1.19	-2.28	0.01	FAM180A	UNQ1940	family with sequence similarity 180 member A
1016	-1.22	-2.32	0.00	CDH18	CDH14	cadherin 18
114798	-1.33	-2.52	0.01	SLITRK1	LRRC12	SLIT and NTRK like family member 1
6335	-1.35	-2.55	0.00	SCN9A	ETHA	sodium voltage-gated channel alpha subunit 9
91851	-1.48	-2.79	0.02	CHRDL1	CHL	chordin like 1
85477	-1.48	-2.79	0.01	SCIN	SCIN	scinderin
2070	-1.59	-3.01	0.03	EYA4	CMD1J	EYA transcriptional coactivator and phosphatase 4
8710	-1.71	-3.28	0.01	SERPINB7	MEGSIN	serpin family B member 7
79853	-1.79	-3.47	0.00	TM4SF20	PRO994	transmembrane 4 L six family member 20
8092	-1.84	-3.59	0.01	ALX1	CART1	ALX homeobox 1
2328	-2.09	-4.25	0.02	FMO3	FMOII	flavin containing dimethylaniline monoxygenase 3

Supplementary Table 3. List of differential expression genes UMDF vs Controls.

Entrez_ gene_id	logFC	FC	P.Value	Symbol	Alias	Gene_name
8076	2.58	5.98	0.02	MFAP5	AAT9	microfibril associated protein 5
1645	2.49	5.60	0.02	AKR1C1	2-ALPHA-HSD	aldo-keto reductase family 1 member C1
6424	2.44	5.41	0.04	SFRP4	FRP-4	secreted frizzled related protein 4
7373	1.58	2.99	0.03	COL14A1	UND	collagen type XIV alpha 1 chain
4916	1.52	2.87	0.01	NTRK3	GP145-TrkC	neurotrophic receptor tyrosine kinase 3
84935	1.40	2.64	0.05	MEDAG	AWMS3	mesenteric estrogen dependent adipogenesis
5318	1.39	2.62	0.01	PKP2	ARVD9	plakophilin 2
3899	1.39	2.62	0.01	AFF3	LAF4	AF4/FMR2 family member 3
5999	1.37	2.58	0.01	RGS4	RGP4	regulator of G protein signaling 4
64097	1.33	2.52	0.01	EPB41L4A	EPB41L4	erythrocyte membrane protein band 4.1 like 4A
100131187	1.24	2.36	0.01	TSTD1	KAT	thiosulfate sulfurtransferase like domain containing 1
22875	1.23	2.35	0.02	ENPP4	NPP4	ectonucleotide pyrophosphatase/phosphodiesterase 4
8470	1.11	2.16	0.01	SORBS2	ARGBP2	sorbin and SH3 domain containing 2
8854	1.07	2.09	0.04	ALDH1A2	RALDH(II)	aldehyde dehydrogenase 1 family member A2
710	1.04	2.05	0.04	SERPING1	C1IN	serpin family G member 1
57608	0.93	1.91	0.03	JCAD	KIAA1462	junctional cadherin 5 associated
4147	0.93	1.90	0.03	MATN2	MATN2	matrilin 2
56967	0.93	1.90	0.00	C14orf132	C14orf88	chromosome 14 open reading frame 132
6913	0.90	1.86	0.05	TBX15	TBX14	T-box transcription factor 15
440993	0.90	1.86	0.03	MIR570HG	LINC00969	MIR570 host gene
55959	0.84	1.79	0.02	SULF2	HSULF-2	sulfatase 2
5212	0.82	1.77	0.04	VIT	VIT1	vitrin
51554	0.80	1.74	0.03	ACKR4	CC-CKR-11	atypical chemokine receptor 4
54749	0.79	1.73	0.04	EPDR1	EPDR	ependymin related 1
28951	0.76	1.69	0.02	TRIB2	C5FW	tribbles pseudokinase 2
126393	0.76	1.69	0.03	HSPB6	HEL55	heat shock protein family B (small) member 6
10659	0.76	1.69	0.02	CELF2	BRUNOL3	CUGBP Elav-like family member 2
58191	0.73	1.66	0.02	CXCL16	CXCLG16	C-X-C motif chemokine ligand 16
1138	0.72	1.65	0.03	CHRNA5	LNCR2	cholinergic receptor nicotinic alpha 5 subunit
27286	0.70	1.62	0.01	SRPX2	BPP	sushi repeat containing protein X-linked 2
3708	0.69	1.61	0.02	ITPR1	ACV	inositol 1.4.5-trisphosphate receptor type 1
23460	0.68	1.60	0.04	ABCA6	EST155051	ATP binding cassette subfamily A member 6
3105	0.63	1.55	0.01	HLA-A	HLAA	major histocompatibility complex. class I. A
57537	0.61	1.53	0.02	SORCS2	SORCS2	sortilin related VPS10 domain containing receptor 2
84674	0.60	1.51	0.04	CARD6	CINCIN1	caspase recruitment domain family member 6
100192204	0.59	1.50	0.01	PPIAP30	PPIAP30	peptidylprolyl isomerase A pseudogene 30
10653	0.58	1.50	0.00	SPINT2	DIAR3	serine peptidase inhibitor. Kunitz type 2
128822	-0.61	-1.52	0.00	CST9	CLM	cystatin 9
6751	-0.62	-1.54	0.03	SSTR1	SRIF-2	somatostatin receptor 1
6335	-0.65	-1.57	0.02	SCN9A	ETHA	sodium voltage-gated channel alpha subunit 9
4951	-0.66	-1.58	0.01	OCM2	OCM	oncomodulin 2
347404	-0.67	-1.59	0.00	LANCL3	LANCL3	LanC like 3
143425	-0.80	-1.74	0.00	SYT9	SYT9	synaptotagmin 9
84302	-0.81	-1.75	0.00	PGAP4	C9orf125	post-GPI attachment to proteins GalNAc transferase 4
864	-0.84	-1.79	0.00	RUNX3	AML2	RUNX family transcription factor 3

Entrez_ gene_id	logFC	FC	P.Value	Symbol	Alias	Gene_name
256691	-0.87	-1.82	0.02	MAMDC2	MAMDC2	MAM domain containing 2
4856	-0.90	-1.87	0.02	CCN3	IBP-9	cellular communication network factor 3
1016	-1.17	-2.25	0.01	CDH18	CDH14	cadherin 18
121601	-1.36	-2.57	0.00	ANO4	TMEM16D	anoctamin 4
338645	-1.80	-3.48	0.05	LUZP2	KFSP2566	leucine zipper protein 2
8076	2.58	5.98	0.02	MFAP5	AAT9	microfibril associated protein 5
1645	2.49	5.60	0.02	AKR1C1	2-ALPHA-HSD	aldo-keto reductase family 1 member C1
6424	2.44	5.41	0.04	SFRP4	FRP-4	secreted frizzled related protein 4
7373	1.58	2.99	0.03	COL14A1	UND	collagen type XIV alpha 1 chain
4916	1.52	2.87	0.01	NTRK3	GP145-TrkC	neurotrophic receptor tyrosine kinase 3
84935	1.40	2.64	0.05	MEDAG	AWMS3	mesenteric estrogen dependent adipogenesis
5318	1.39	2.62	0.01	PKP2	ARVD9	plakophilin 2
3899	1.39	2.62	0.01	AFF3	LAF4	AF4/FMR2 family member 3
5999	1.37	2.58	0.01	RGS4	RGP4	regulator of G protein signaling 4
64097	1.33	2.52	0.01	EPB41L4A	EPB41L4	erythrocyte membrane protein band 4.1 like 4A
100131187	1.24	2.36	0.01	TSTD1	KAT	thiosulfate sulfurtransferase like domain containing 1
22875	1.23	2.35	0.02	ENPP4	NPP4	ectonucleotide pyrophosphatase/phosphodiesterase 4
8470	1.11	2.16	0.01	SORBS2	ARGBP2	sorbin and SH3 domain containing 2
8854	1.07	2.09	0.04	ALDH1A2	RALDH(II)	aldehyde dehydrogenase 1 family member A2
710	1.04	2.05	0.04	SERPING1	C1IN	serpin family G member 1
57608	0.93	1.91	0.03	JCAD	KIAA1462	junctional cadherin 5 associated
4147	0.93	1.90	0.03	MATN2	MATN2	matrilin 2
56967	0.93	1.90	0.00	C14orf132	C14orf88	chromosome 14 open reading frame 132
6913	0.90	1.86	0.05	TBX15	TBX14	T-box transcription factor 15
440993	0.90	1.86	0.03	MIR570HG	LINC00969	MIR570 host gene
55959	0.84	1.79	0.02	SULF2	HSULF-2	sulfatase 2
5212	0.82	1.77	0.04	VIT	VIT1	vitrin
51554	0.80	1.74	0.03	ACKR4	CC-CKR-11	atypical chemokine receptor 4
54749	0.79	1.73	0.04	EPDR1	EPDR	ependymin related 1
28951	0.76	1.69	0.02	TRIB2	C5FW	tribbles pseudokinase 2
126393	0.76	1.69	0.03	HSPB6	HEL55	heat shock protein family B (small) member 6
10659	0.76	1.69	0.02	CELF2	BRUNOL3	CUGBP Elav-like family member 2
58191	0.73	1.66	0.02	CXCL16	CXCLG16	C-X-C motif chemokine ligand 16
1138	0.72	1.65	0.03	CHRNA5	LNCR2	cholinergic receptor nicotinic alpha 5 subunit
27286	0.70	1.62	0.01	SRPX2	BPP	sushi repeat containing protein X-linked 2
3708	0.69	1.61	0.02	ITPR1	ACV	inositol 1.4.5-trisphosphate receptor type 1
23460	0.68	1.60	0.04	ABCA6	EST155051	ATP binding cassette subfamily A member 6
3105	0.63	1.55	0.01	HLA-A	HLAA	major histocompatibility complex. class I. A
57537	0.61	1.53	0.02	SORCS2	SORCS2	sortilin related VPS10 domain containing receptor 2
84674	0.60	1.51	0.04	CARD6	CINCIN1	caspase recruitment domain family member 6
100192204	0.59	1.50	0.01	PPIAP30	PPIAP30	peptidylprolyl isomerase A pseudogene 30
10653	0.58	1.50	0.00	SPINT2	DIAR3	serine peptidase inhibitor. Kunitz type 2
128822	-0.61	-1.52	0.00	CST9	CLM	cystatin 9
6751	-0.62	-1.54	0.03	SSTR1	SRIF-2	somatostatin receptor 1
6335	-0.65	-1.57	0.02	SCN9A	ETHA	sodium voltage-gated channel alpha subunit 9
4951	-0.66	-1.58	0.01	OCM2	OCM	oncomodulin 2

Entrez_ gene_id	logFC	FC	P.Value	Symbol	Alias	Gene_name
347404	-0.67	-1.59	0.00	LANCL3	LANCL3	LanC like 3
143425	-0.80	-1.74	0.00	SYT9	SYT9	synaptotagmin 9
84302	-0.81	-1.75	0.00	PGAP4	C9orf125	post-GPI attachment to proteins GalNAc transferase 4
864	-0.84	-1.79	0.00	RUNX3	AML2	RUNX family transcription factor 3
256691	-0.87	-1.82	0.02	MAMDC2	MAMDC2	MAM domain containing 2
4856	-0.90	-1.87	0.02	CCN3	IBP-9	cellular communication network factor 3
1016	-1.17	-2.25	0.01	CDH18	CDH14	cadherin 18
121601	-1.36	-2.57	0.00	ANO4	TMEM16D	anoctamin 4
338645	-1.80	-3.48	0.05	LUZP2	KFSP2566	leucine zipper protein 2
8076	2.58	5.98	0.02	MFAP5	AAT9	microfibril associated protein 5
1645	2.49	5.60	0.02	AKR1C1	2-ALPHA-HSD	aldo-keto reductase family 1 member C1
6424	2.44	5.41	0.04	SFRP4	FRP-4	secreted frizzled related protein 4
7373	1.58	2.99	0.03	COL14A1	UND	collagen type XIV alpha 1 chain
4916	1.52	2.87	0.01	NTRK3	GP145-TrkC	neurotrophic receptor tyrosine kinase 3
84935	1.40	2.64	0.05	MEDAG	AWMS3	mesenteric estrogen dependent adipogenesis
5318	1.39	2.62	0.01	PKP2	ARVD9	plakophilin 2
3899	1.39	2.62	0.01	AFF3	LAF4	AF4/FMR2 family member 3
5999	1.37	2.58	0.01	RGS4	RGP4	regulator of G protein signaling 4
64097	1.33	2.52	0.01	EPB41L4A	EPB41L4	erythrocyte membrane protein band 4.1 like 4A
100131187	1.24	2.36	0.01	TSTD1	KAT	thiosulfate sulfurtransferase like domain containing 1
22875	1.23	2.35	0.02	ENPP4	NPP4	ectonucleotide pyrophosphatase/phosphodiesterase 4
8470	1.11	2.16	0.01	SORBS2	ARGBP2	sorbin and SH3 domain containing 2
8854	1.07	2.09	0.04	ALDH1A2	RALDH(II)	aldehyde dehydrogenase 1 family member A2
710	1.04	2.05	0.04	SERPING1	C1IN	serpin family G member 1
57608	0.93	1.91	0.03	JCAD	KIAA1462	junctional cadherin 5 associated
4147	0.93	1.90	0.03	MATN2	MATN2	matrilin 2
56967	0.93	1.90	0.00	C14orf132	C14orf88	chromosome 14 open reading frame 132
6913	0.90	1.86	0.05	TBX15	TBX14	T-box transcription factor 15
440993	0.90	1.86	0.03	MIR570HG	LINC00969	MIR570 host gene
55959	0.84	1.79	0.02	SULF2	HSULF-2	sulfatase 2
5212	0.82	1.77	0.04	VIT	VIT1	vitrin
51554	0.80	1.74	0.03	ACKR4	CC-CKR-11	atypical chemokine receptor 4
54749	0.79	1.73	0.04	EPDR1	EPDR	ependymin related 1
28951	0.76	1.69	0.02	TRIB2	C5FW	tribbles pseudokinase 2
126393	0.76	1.69	0.03	HSPB6	HEL55	heat shock protein family B (small) member 6
10659	0.76	1.69	0.02	CELF2	BRUNOL3	CUGBP Elav-like family member 2
58191	0.73	1.66	0.02	CXCL16	CXCLG16	C-X-C motif chemokine ligand 16
1138	0.72	1.65	0.03	CHRNA5	LNCR2	cholinergic receptor nicotinic alpha 5 subunit
27286	0.70	1.62	0.01	SRPX2	BPP	sushi repeat containing protein X-linked 2
3708	0.69	1.61	0.02	ITPR1	ACV	inositol 1.4.5-trisphosphate receptor type 1
23460	0.68	1.60	0.04	ABCA6	EST155051	ATP binding cassette subfamily A member 6
3105	0.63	1.55	0.01	HLA-A	HLAA	major histocompatibility complex. class I. A
57537	0.61	1.53	0.02	SORCS2	SORCS2	sortilin related VPS10 domain containing receptor 2
84674	0.60	1.51	0.04	CARD6	CINCIN1	caspase recruitment domain family member 6
100192204	0.59	1.50	0.01	PPIAP30	PPIAP30	peptidylprolyl isomerase A pseudogene 30
10653	0.58	1.50	0.00	SPINT2	DIAR3	serine peptidase inhibitor. Kunitz type 2

Entrez_ gene_id	logFC	FC	P.Value	Symbol	Alias	Gene_name
128822	-0.61	-1.52	0.00	CST9	CLM	cystatin 9
6751	-0.62	-1.54	0.03	SSTR1	SRIF-2	somatostatin receptor 1
6335	-0.65	-1.57	0.02	SCN9A	ETHA	sodium voltage-gated channel alpha subunit 9
4951	-0.66	-1.58	0.01	OCM2	OCM	oncomodulin 2
347404	-0.67	-1.59	0.00	LANCL3	LANCL3	LanC like 3
143425	-0.80	-1.74	0.00	SYT9	SYT9	synaptotagmin 9
84302	-0.81	-1.75	0.00	PGAP4	C9orf125	post-GPI attachment to proteins GalNAc transferase 4
864	-0.84	-1.79	0.00	RUNX3	AML2	RUNX family transcription factor 3
256691	-0.87	-1.82	0.02	MAMDC2	MAMDC2	MAM domain containing 2
4856	-0.90	-1.87	0.02	CCN3	IBP-9	cellular communication network factor 3
1016	-1.17	-2.25	0.01	CDH18	CDH14	cadherin 18
121601	-1.36	-2.57	0.00	ANO4	TMEM16D	anoctamin 4
338645	-1.80	-3.48	0.05	LUZP2	KFSP2566	leucine zipper protein 2

Supplementary Table 4. List of differential expression genes NPDF vs UMDF.

Entrez_ gene_id	logFC	FC	P.Value	Symbol	Alias	Gene_name
3815	1.59	3.00	0.01	KIT	C-Kit	KIT proto-oncogene. receptor tyrosine kinase
953	1.51	2.85	0.00	ENTPD1	ATPDase	ectonucleoside triphosphate diphosphohydrolase 1
7092	1.47	2.77	0.00	TLL1	ASD6	tolloid like 1
684	1.34	2.53	0.01	BST2	CD317	bone marrow stromal cell antigen 2
4081	1.34	2.53	0.03	MAB21L1	CAGR1	mab-21 like 1
56892	1.26	2.39	0.00	TCIM	C8orf4	transcriptional and immune response regulator
10402	1.18	2.27	0.03	ST3GAL6	SIAT10	ST3 beta-galactoside alpha-2.3-sialyltransferase 6
864	1.07	2.11	0.00	RUNX3	AML2	RUNX family transcription factor 3
9076	0.95	1.94	0.00	CLDN1	CLD1	claudin 1
5099	0.92	1.89	0.02	PCDH7	BH-Pcdh	protocadherin 7
23284	0.92	1.89	0.02	ADGRL3	CIRL3	adhesion G protein-coupled receptor L3
10125	0.85	1.81	0.03	RASGRP1	CALDAG-GEFI	RAS guanyl releasing protein 1
8972	0.84	1.79	0.02	MGAM	MG	maltase-glucoamylase
8835	0.84	1.79	0.01	SOCS2	CIS2	suppressor of cytokine signaling 2
5649	0.83	1.77	0.03	RELN	ETL7	reelin
182	0.82	1.77	0.03	JAG1	AGS	jagged canonical Notch ligand 1
286183	0.82	1.77	0.00	NKAIN3	FAM77D	sodium/potassium transporting ATPase interacting 3
100507421	0.80	1.74	0.01	TMEM178B	TMEM178B	transmembrane protein 178B
8436	0.78	1.72	0.00	CAVIN2	PS-p68	caveolae associated protein 2
121601	0.77	1.71	0.00	ANO4	TMEM16D	anoctamin 4
397	0.74	1.67	0.04	ARHGDIB	D4	Rho GDP dissociation inhibitor beta
5069	0.74	1.67	0.00	PAPPA	ASBABP2	pappalysin 1
1839	0.73	1.66	0.01	HBEGF	DTR	heparin binding EGF like growth factor
9586	0.71	1.64	0.03	CREB5	CRE-BPA	cAMP responsive element binding protein 5
6792	0.71	1.64	0.03	CDKL5	CFAP247	cyclin dependent kinase like 5
4325	0.70	1.63	0.04	MMP16	C8orf57	matrix metallopeptidase 16

Entrez_ gene_id	logFC	FC	P.Value	Symbol	Alias	Gene_name
2201	0.69	1.61	0.01	FBN2	CCA	fibrillin 2
128553	0.69	1.61	0.04	TSHZ2	C20orf17	teashirt zinc finger homeobox 2
50863	0.68	1.61	0.01	NTM	CEPU-1	neurotrimin
1829	0.68	1.61	0.03	DSG2	CDHF5	desmoglein 2
152330	0.67	1.60	0.03	CNTN4	AXCAM	contactin 4
84553	0.67	1.60	0.00	FAXC	C6orf168	failed axon connections homolog. metaxin like GST domain containing
10085	0.67	1.59	0.05	EDIL3	DEL1	EGF like repeats and discoidin domains 3
23043	0.66	1.58	0.05	TNIK	MRT54	TRAF2 and NCK interacting kinase
3690	0.64	1.56	0.01	ITGB3	BDPLT16	integrin subunit beta 3
1301	0.64	1.56	0.04	COL11A1	CO11A1	collagen type XI alpha 1 chain
23705	0.63	1.55	0.02	CADM1	BL2	cell adhesion molecule 1
5734	0.63	1.54	0.03	PTGER4	EP4	prostaglandin E receptor 4
55784	0.63	1.54	0.04	MCTP2	MCTP2	multiple C2 and transmembrane domain containing 2
4599	0.61	1.53	0.05	MX1	IFI-78K	MX dynamin like GTPase 1
55824	0.60	1.52	0.00	PAG1	CBP	phosphoprotein membrane anchor with glycosphingolipid microdomains 1
93145	0.60	1.52	0.02	OLFM2	NOE2	olfactomedin 2
3556	0.58	1.49	0.02	IL1RAP	C3orf13	interleukin 1 receptor accessory protein
9495	0.57	1.48	0.00	AKAP5	AKAP75	A-kinase anchoring protein 5
1295	0.56	1.48	0.04	COL8A1	C3orf7	collagen type VIII alpha 1 chain
51301	0.56	1.48	0.04	GCNT4	C2GNT3	glucosaminyl (N-acetyl) transferase 4
221687	0.55	1.46	0.02	RNF182	RNF182	ring finger protein 182
107987150	0.54	1.46	0.01	LOC107987150	LOC107987150	uncharacterized LOC107987150
26353	0.54	1.46	0.02	HSPB8	CMT2L	heat shock protein family B (small) member 8
166647	0.54	1.45	0.01	ADGRA3	GPR125	adhesion G protein-coupled receptor A3
9891	0.53	1.45	0.05	NUAK1	ARK5	NUAK family kinase 1
2775	0.53	1.45	0.00	GNAO1	EIEE17	G protein subunit alpha o1
2890	0.53	1.44	0.01	GRIA1	GLUH1	glutamate ionotropic receptor AMPA type subunit 1
28951	0.52	1.44	0.02	TRIB2	C5FW	tribbles pseudokinase 2
4254	0.52	1.43	0.01	KITLG	DCUA	KIT ligand
5241	0.52	1.43	0.02	PGR	NR3C3	progesterone receptor
57713	0.52	1.43	0.01	SFMBT2	SFMBT2	Scm like with four mbt domains 2
107985780	0.51	1.43	0.01	LOC107985780	LOC107985780	uncharacterized LOC107985780
23670	0.51	1.43	0.00	CEMIP2	TMEM2	cell migration inducing hyaluronidase 2
4978	0.51	1.42	0.00	OPCML	IGLON1	opioid binding protein/cell adhesion molecule like
3764	0.51	1.42	0.03	KCNJ8	KIR6.1	potassium inwardly rectifying channel subfamily J member 8
5738	0.50	1.41	0.01	PTGFRN	CD315	prostaglandin F2 receptor inhibitor
6983	-0.58	-1.50	0.01	TRGV9	TCRGV9	T cell receptor gamma variable 9
1634	-0.59	-1.50	0.02	DCN	CSCD	decorin
54947	-0.60	-1.51	0.02	LPCAT2	AGPAT11	lysophosphatidylcholine acyltransferase 2
100533183	-0.61	-1.52	0.01	ZNF664-RFLNA	ZNF664-RFLNA	ZNF664-RFLNA readthrough
2048	-0.63	-1.54	0.00	EPHB2	BDPLT22	EPH receptor B2
2702	-0.64	-1.56	0.01	GJA5	ATFB11	gap junction protein alpha 5
1396	-0.65	-1.56	0.01	CRIP1	CRHP	cysteine rich protein 1
1397	-0.65	-1.57	0.02	CRIP2	CRIP	cysteine rich protein 2
6586	-0.66	-1.58	0.03	SLIT3	MEGF5	slit guidance ligand 3

Entrez_ gene_id	logFC	FC	P.Value	Symbol	Alias	Gene_name
9244	-0.67	-1.59	0.03	CRLF1	CISS	cytokine receptor like factor 1
6335	-0.70	-1.62	0.00	SCN9A	ETHA	sodium voltage-gated channel alpha subunit 9
389558	-0.70	-1.62	0.03	FAM180A	UNQ1940	family with sequence similarity 180 member A
1382	-0.71	-1.63	0.04	CRABP2	CRABP-II	cellular retinoic acid binding protein 2
79974	-0.72	-1.65	0.02	CPED1	C7orf58	cadherin like and PC-esterase domain containing 1
7164	-0.73	-1.66	0.00	TPD52L1	D53	TPD52 like 1
147463	-0.74	-1.67	0.03	ANKRD29	ANKRD29	ankyrin repeat domain 29
2170	-0.75	-1.68	0.02	FABP3	FABP11	fatty acid binding protein 3
56479	-0.75	-1.68	0.01	KCNQ5	Kv7.5	potassium voltage-gated channel subfamily Q member 5
113146	-0.76	-1.70	0.02	AHNAK2	C14orf78	AHNAK nucleoprotein 2
4237	-0.78	-1.72	0.03	MFAP2	MAGP	microfibril associated protein 2
22875	-0.79	-1.73	0.04	ENPP4	NPP4	ectonucleotide pyrophosphatase/phosphodiesterase 4
5157	-0.79	-1.73	0.04	PDGFRL	PDGRL	platelet derived growth factor receptor like
9079	-0.79	-1.73	0.02	LDB2	CLIM1	LIM domain binding 2
9365	-0.83	-1.78	0.01	KL	HFTC3	klotho
6405	-0.86	-1.81	0.00	SEMA3F	SEMA-IV	semaphorin 3F
51554	-0.86	-1.81	0.00	ACKR4	CC-CKR-11	atypical chemokine receptor 4
23643	-0.91	-1.88	0.00	LY96	ESOP-1	lymphocyte antigen 96
9182	-0.92	-1.90	0.02	RASSF9	P-CIP1	Ras association domain family member 9
54756	-0.95	-1.93	0.04	IL17RD	HH18	interleukin 17 receptor D
54829	-1.00	-2.01	0.00	ASPN	OS3	asporin
287	-1.03	-2.04	0.02	ANK2	ANK-2	ankyrin 2
374462	-1.07	-2.10	0.00	PTPRQ	DFNA73	protein tyrosine phosphatase receptor type Q
1368	-1.15	-2.22	0.04	CPM	CPM	carboxypeptidase M
92949	-1.18	-2.26	0.00	ADAMTSL1	ADAMTSL-1	ADAMTS like 1
79853	-1.18	-2.27	0.00	TM4SF20	PRO994	transmembrane 4 L six family member 20
5081	-1.20	-2.30	0.01	PAX7	HUP1	paired box 7
8710	-1.22	-2.32	0.02	SERPINB7	MEGSIN	serpin family B member 7
2326	-1.39	-2.63	0.03	FMO1	FMO1	flavin containing dimethylaniline monoxygenase 1
8092	-1.58	-2.98	0.00	ALX1	CART1	ALX homeobox 1
4958	-1.62	-3.07	0.02	OMD	OSAD	osteomodulin
2070	-1.73	-3.33	0.00	EYA4	CMD1J	EYA transcriptional coactivator and phosphatase 4
91851	-2.02	-4.05	0.00	CHRDL1	CHL	chordin like 1
8076	-2.12	-4.35	0.01	MFAP5	AAT9	microfibril associated protein 5